

The Water-Exchange Mechanism of the $[\text{UO}_2(\text{OH}_2)_5]^{2+}$ Ion Revisited: The Importance of a Proper Treatment of Electron Correlation

François P. Rotzinger*^[a]

Dedicated to Professor André E. Merbach on the occasion of his 65th birthday

Abstract: The water-exchange mechanism of $[\text{UO}_2(\text{OH}_2)_5]^{2+}$ has been reinvestigated by using ab initio molecular orbital (MO) methods. The geometries and the vibrational frequencies were computed with CAS-SCF(12/11)-SCRF and CAS-SCF(12/11)-PCM methods, which take into account static electron correlation (using the complete active space self-consistent field (CAS-SCF) technique, based on an active space of 12 electrons in 11 orbitals) and hydration (using the self-consistent reaction field (SCRF) and polarizable continuum model (PCM) techniques). The total energies were computed with multiconfiguration quasi-degenerate

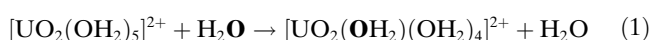
second-order perturbation theory, the MCQDPT2(12/11)-PCM method, which treats static and dynamic electron correlation as well as hydration. The adequacies of other currently used quantum chemical methods, MP2, CCSD(T), B3LYP, and BLYP, are discussed. For the associative and dissociative pathways, thermodynamic activation parameters (ΔH^\ddagger , ΔS^\ddagger , and ΔG^\ddagger) were computed. For the associa-

tive mechanism, the calculated ΔH^\ddagger and ΔG^\ddagger values agree with experiment, whereas for the dissociative mechanism, they are higher by $\approx 20 \text{ kJ mol}^{-1}$. The dissociative mechanism is preferred for substitution reactions of uranyl(VI) complexes with ligands that are stronger electron donors than water. The question of whether a concerted (I_a or I_d) or a stepwise (A or D) mechanism operates is discussed on the basis of the computed lifetime of the respective intermediate, and the duration of the vibration with which the intermediate is transformed into the product.

Keywords: ab initio calculations • ligand effects • quantum chemical calculations • substitution mechanisms • uranium • water chemistry

Introduction

The kinetics of the water-exchange reaction [Eq. (1)] of the $[\text{UO}_2(\text{OH}_2)_5]^{2+}$ ion have been investigated by Farkas et al.^[1] in a variable-temperature ^{17}O NMR study.



They determined the activation parameters (ΔH^\ddagger , ΔS^\ddagger , and ΔG^\ddagger) at 25 °C, but not the activation volume (ΔV^\ddagger). For the assignment of the exchange mechanism, they resorted to quantum chemical computations based on a model^[2] involving constrained optimizations, which is known^[3,4] to favor the dissociative pathway. Not unexpectedly, they postulated a dissociative mechanism for the reaction shown in Equation (1). In a second study^[5] on this reaction from the same laboratory, an improved model^[3,4] was used, and hydration was treated on the basis of the conductor polarizable continuum model (CPCM).^[6–9] In contrast to the first investigation,^[1] the associative (A) mechanism, proceeding through the $[\text{UO}_2(\text{OH}_2)_6]^{2+}$ intermediate with an increased coordination number, was claimed to operate, because it was found to be more thermodynamically advantageous, by $\approx 40 \text{ kJ mol}^{-1}$, than the dissociative (D) pathway, which involves the $[\text{UO}_2(\text{OH}_2)_4]^{2+}$ intermediate exhibiting a reduced

[a] PD Dr. F. P. Rotzinger
Institut des Sciences et Ingénierie Chimiques
Ecole Polytechnique Fédérale de Lausanne (EPFL)
Station 6, 1015 Lausanne (Switzerland)
Fax (+41)21-693-4111
E-mail: francois.rotzinger@epfl.ch

Supporting Information for this article available on the WWW under <http://www.chemeurj.org> or from the author: Tables S1–S6 list the atomic coordinates of the species involved in Equations (3) and (4) (CAS-SCF(12/11)-SCRF/PCM geometries), and Figures S1 and S2 represent a perspective view thereof together with the imaginary mode of the transition states. A detailed description of the configuration interaction (CI) calculations for the determination of the active space is given in the Appendix.

coordination number. Very recently, this reaction [Eq. (1)] was reinvestigated^[10] by using constrained Car–Parrinello molecular dynamics simulations (CPMD)^[11] based on the BLYP^[12–14] functional. For the D mechanism, an activation free energy (ΔA^\ddagger) of 45.2 kJ mol⁻¹ was obtained (at 27 °C), which is ≈ 7 kJ mol⁻¹ higher than the experimental ΔG^\ddagger value (at 25 °C).^[1] For the associative mechanism, a lower ΔA^\ddagger (28.0 kJ mol⁻¹) was found, which is 10 kJ mol⁻¹ lower than that found by experiment.

In addition to reaction (1), Vallet et al. studied the water-exchange reaction of the bisoxalato aqua dioxouranium(VI) complex, $[\text{UO}_2(\text{C}_2\text{O}_4)_2\text{OH}_2]^{2-}$, which was claimed to proceed by means of the A mechanism^[5] as for $[\text{UO}_2(\text{OH}_2)_5]^{2+}$. In a later investigation from the same laboratory,^[15] the water-exchange reaction of the similar tetrafluoro aqua dioxouranium(VI) complex, $[\text{UO}_2\text{F}_4(\text{OH}_2)]^{2-}$, exhibiting the same charge as the bisoxalato dioxouranium(VI) ion, was claimed to proceed through the D mechanism. It is incomprehensible that the rather similar oxalato and fluoro complexes should undergo the water-exchange process with opposite mechanisms. Thus, the substitution mechanism of these UO_2^{2+} complexes cannot be considered as fully understood. It will be shown that computational methods, the applicability of which was not verified, were used in these UO_2^{2+} studies;^[1,5,15] thus the quality of the computed activation energies is not established. Evidently, the preferred reaction mechanism, associative or dissociative, cannot be predicted on the basis of such data.

For the computation of activation energies of reactions in solution, solvation and electron correlation have to be treated adequately. In the first study of reaction (1) by Farkas et al.,^[1] the geometries were optimized using the Hartree–Fock (HF) procedure for the free ions in the gas phase, and the energies were computed with MP2, also for the free ions. Static electron correlation, which is present in the UO_2^{2+} ion as in all metal-oxo complexes, such as the $[\text{VO}(\text{OH}_2)_5]^{2+}$ complex^[16], was neglected in both the geometry optimizations and the energy computations. It is important to note that MP2 involves configurations with excitations of up to two electrons. Therefore MP2 should only be applied if the contribution of configurations arising from excitations of more than two electrons is negligible, and if the perturbation is small, otherwise static electron correlation is present. In such cases, the zero-order HF wavefunction is not a sufficiently good approximation and single-reference perturbation theory based on excitations of up to two electrons is inappropriate.^[16]

The second quantum chemical study of reaction (1) from the same laboratory by Vallet et al.^[5] was again based on HF geometries and MP2 energies, although hydration was treated with CPCM.^[6–9] In this investigation too, static electron correlation, which arises from the population of $\sigma^*(\text{O}=\text{U}=\text{O})$ and $\pi^*(\text{O}=\text{U}=\text{O})$ molecular orbitals (MOs) by $\sigma(\text{O}=\text{U}=\text{O})$ and $\pi(\text{O}=\text{U}=\text{O})$ electrons (see Computational Methods and Results sections) was neglected. The authors did not assess the validity of these approximations. As shown re-

cently,^[16,17] the inappropriate treatment of electron correlation can lead to incorrect conclusions.

The result of the very recent CPMD studies^[10] of reaction (1), in which the solvent was treated quantum chemically, might be affected by the limitations of density function theory (DFT). At least for aqua ions, DFT favors systematically the lower coordination number,^[16] and this is the reason that, for example, B3LYP^[18–20] and BLYP^[12–14] give rise to a preference for the dissociative mechanism together with a discrimination of the associative pathway. These CPMD calculations,^[10] based on the BLYP functional, might underestimate the activation energy for the D mechanism, but, in contrast to the above-mentioned cases,^[16] they underestimate the activation energy for the associative pathway as well. In fact, in the first CPMD study,^[10a] the authors made the statement “Arguably, the largest uncertainty arises from the particular quantum chemical method employed, BLYP in our case.” This, however, was supported neither by data nor by a reference, although such information was available from the literature.^[16]

With DFT, the structure of the transition state $[\text{cis-V}(\text{OH}_2)_5\cdots(\text{OH}_2)_2]^{2+\ddagger}$ cannot be obtained because the weak metal–aqua and hydrogen bonds are not balanced correctly.^[16] Furthermore, the geometry of the water adducts $[\text{M}(\text{OH}_2)_6\text{OH}_2]^{3+}$, in which the seventh H_2O is bound to the first coordination sphere by means of a single hydrogen bond, cannot be computed with DFT because of a spontaneous H^+ transfer from the first to the second coordination sphere, which leads to $[\text{M}(\text{OH}_2)_5\text{OH}\cdot\text{H}_3\text{O}]^{3+}$.^[16] Reaction (1) is a textbook example illustrating that computed properties can depend critically on the treatment of electron correlation.

The present study on reaction (1) is performed with quantum chemical methods that take into account static and dynamic electron correlation. The systematic deviations in activation and reaction energies, which were obtained with HF and post-HF methods (MP2, CCSD(T),^[21] MCQDPT2,^[22,23]) on one hand, and DFT (B3LYP, BLYP) on the other hand, are illustrated. The effect of quantum chemical methods for geometry optimization and energy computation on the energetics and, therefore, the mechanism of reaction (1), is demonstrated. The activation parameters for the A and D mechanisms, computed at 25 °C, are compared with the experimental data. The activation enthalpy (ΔH^\ddagger) and free enthalpy (ΔG^\ddagger) for the A mechanism agree with experiment. The D mechanism is less likely, since its ΔG^\ddagger is higher by at least 15 kJ mol⁻¹. The lifetime of the intermediates for the A and the D mechanisms was computed to be short. Criteria for the distinction of the stepwise (A and D) from the concerted (I_a and I_d) mechanisms are presented. The present data allows the rationalization of the reactivity of UO_2^{2+} complexes and the attribution of their preferred water-exchange mechanisms.

Computational Methods

All of the calculations were performed using the GAMESS^[24] programs. For uranium, the relativistic effective core potential (ECP) basis set of Hay and Martin^[25] was used, in which the 1s–5s, 2p–5p, 3d–5d, and 4f shells are included in the relativistic core, and the 6s, 7s, 6p, 7p, 6d, and 5f shells are represented by a (10s, 8p, 2d, 4f) basis set contracted to [3s, 3p, 2d, 2f]. For O and H, the 6–31G(d) basis set^[26,27] was used ($\alpha_d = 1.20$ ^[28]), which was shown to be adequate for water and oxo ligands.^[16] To determine the effect of p polarization functions on the H atoms, computations with a 6–31G(d,p) basis set for H₂O ($\alpha_p = 0.80$ ^[28]) were performed. Figures 1–3 were generated with Molden,^[29] and Figures S1 and S2 (Supporting Information) were plotted using the graphics programs of GAMESS.^[24]

The Hessians were calculated numerically (with analytical gradients) using the double difference method, and projected to eliminate rotational and translational contaminants.^[30] The thermodynamic variables (ΔH^\ddagger , ΔS^\ddagger , and ΔG^\ddagger) at 25 °C were computed on the basis of statistical mechanics.^[31] Unscaled CAS-SCF(12/11)-SCRF or CAS-SCF(12/11)-PCM frequencies were used for the calculation of the vibrational partition functions. The DFT calculations (B3LYP and BLYP) were performed with a grid finer than the default (NTHE=24 and NPFI=48; the default is NTHE=12 and NPFI=24). The computed vibrational spectrum of transition states exhibited a single imaginary frequency, whereas for the other species, all of the calculated frequencies were real.

The active MOs for the complete active space self-consistent field (CAS-SCF) wavefunctions were determined with configuration interaction (CI) using the iterative natural orbital (INO) method.^[32] The details of the computations for $[\text{UO}_2(\text{OH}_2)_5]^{2+}$ are given in the Appendix (see the Supporting Information). Thus, apart from one exception, all of the CAS-SCF and MCQDPT2 calculations were based on an active space of 12 electrons in 11 orbitals (12/11). In the post-HF calculations (MP2, CCSD(T), and MCQDPT2), the 1s MOs of oxygen were treated as frozen cores.

For the geometry optimizations, which were all performed at the CAS-SCF level, hydration was included using the self-consistent reaction field (SCRF)^[33–35] model with a spherical cavity. It included monopole–dipole and dipole–dipole solute–solvent interactions. The cavity radius was determined as described.^[36] It should be noted that for molecules without permanent dipole moments, the SCRF geometry is equal to that of the free ion in the gas phase. The geometries were further optimized on the basis of a more elaborate treatment of hydration, using the polarizable continuum model (PCM),^[6–8,37] whereby a covalent radius of 2.50 Å was taken for U. Geometry optimizations based on PCM require the use of C₁ symmetry, and for the geometry optimizations, but not the energy computations, a finer tessellation had to be used (NTSALL=240, the default is 60; in PCM, each atom is represented by a sphere, which is approximated by NTSALL triangles). The energies were calculated (using NTSALL=60) at the MCQDPT2^[22,23] level, whereby hydration was treated with PCM as described.^[36] For the presently used (12/11) active space, the computed geometries and energies are denoted as CAS-SCF(12/11)-SCRF/PCM and MCQDPT2(12/11)-PCM, respectively. The atomic coordinates of all species, the geometries and frequencies of which were computed at the CAS-SCF(12/11)-SCRF/PCM level, are given in Tables S1–S6 (Supporting Information).

Results

Dependence of activation and reaction energies on the computational method: The striking differences in activation and reaction energies that are obtained with various computational methods are illustrated in Table 1. The energies were calculated based on the gas-phase geometries of Vallet et al.^[5], whereby a different basis set^[25] was used for urani-

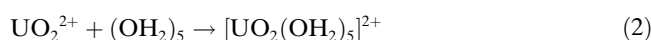
Table 1. Gas-phase activation or reaction energies^[a] calculated on the basis of the Hartree–Fock gas-phase geometries of Vallet et al.^[5]

Reaction	HF	MP2	CCSD(T)	MCQDPT2 ^[b]	B3LYP	BLYP
$[\text{UO}_2(\text{OH}_2)_5]^{2+} \rightarrow [\text{UO}_2(\text{OH}_2)_4 \cdots \text{OH}_2]^{2+\ddagger}$ (activation energy for the D mechanism)	37.8	39.2	39.8	39.3	25.0	17.7
$[\text{UO}_2(\text{OH}_2)_5 \cdots \text{OH}_2]^{2+\ddagger} \rightarrow [\text{UO}_2(\text{OH}_2)_4 \cdots (\text{OH}_2)_2]^{2+\ddagger}$ ^[c] (energy of the intermediate for the A mechanism)	35.7	35.2	32.7	35.9	40.7	40.7
$[\text{UO}_2(\text{OH}_2)_5 \cdots \text{OH}_2]^{2+\ddagger} \rightarrow [\text{UO}_2(\text{OH}_2)_4 \cdots (\text{OH}_2)_2]^{2+}$ (energy of the intermediate for the D mechanism)	44.4	46.2	47.0	46.1	29.0	20.7

[a] Units: kJ mol⁻¹. [b] Second-order perturbation calculation based on the CAS-SCF(12/11) wave function. [c] The nature of this species depends on the U basis set: according to the calculations of Vallet et al.,^[5] this species is a transition state (for the I mechanism), whereas it is an intermediate on the basis of the work of Hay et al.^[38] and the present computations, which have both been performed with the U basis set of Hay and Martin.^[25]

um. Multiconfiguration quasi-degenerate second-order perturbation theory (MCQDPT2),^[22,23] which takes into account static and dynamic electron correlation, as well as coupled-cluster methods, are expected to yield the most accurate energies (see Electron Correlation in Dioxouranium(VI) Complexes section). It can be seen that the HF data are, fortuitously, quite close to MCQDPT2. Due to the presence of static electron correlation, it is uncertain whether (single-reference) MP2 is adequate. Recently, Cao and Balasubramian^[39] investigated, among other things, the dependence of the U=O and U–O bond lengths in $[\text{UO}_2(\text{OH}_2)_n]^{2+}$ ($n = 0, 4–6$) complexes on the computational methods B3LYP, MP2, and CCSD. The B3LYP and CCSD (gas-phase) geometries are quite similar, whereas considerably longer U=O bonds (0.04–0.05 Å longer) and shorter U–O bonds were obtained with MP2. A possible reason why MP2 could nevertheless yield energies close to MCQDPT2 and CCSD(T) is given in the Discussion section. It should be noted that the B3LYP and BLYP energies deviate strongly from those obtained with high-level ab initio methods as seen^[16] for other aqua ions.

Basis set superposition error (BSSE): This error was calculated by using the counterpoise method.^[40] The BSSE of one U–OH₂ bond in $[\text{UO}_2(\text{OH}_2)_5]^{2+}$ was computed with currently used quantum chemical methods (Table 2) for the process shown in Equation (2).



It is interesting to note that MCQDPT2 gives rise to a small-

Table 2. Basis set superposition error (BSSE) of an $\text{U}\cdots\text{OH}_2$ bond in $[\text{UO}_2(\text{OH}_2)_5]^{2+}$.

Method	BSSE ^[a] [kJ mol ⁻¹]	Method	BSSE ^[a] [kJ mol ⁻¹]
HF	9.3	MP2	18.9
CCSD(T)	19.4	MCQDPT2 ^[b]	16.5
B3LYP	11.4	BLYP	13.1

[a] These calculations were performed for the CAS-SCF(12/11)-SCRF geometry. [b] Second-order perturbation calculation based on the CAS-SCF(12/11) wave function.

er BSSE than the post-HF techniques MP2 and CCSD(T), and that DFT lies between HF and MCQDPT2. Irrespective of the mechanism of reaction (1), two major BSSE contributions have to be considered. The first involves the BSSE correction due to bond formation (or breaking), and the second BSSE correction arises from the slight elongation (or shortening) of the “spectator” H_2O ligand bonds, which do not participate in the exchange process. It will be shown below (see Mechanism of the Water-Exchange Reaction of $[\text{UO}_2(\text{OH}_2)_5]^{2+}$ section), that the BSSE is virtually constant for the present reactions: for the example of the A mechanism, the BSSE arising from the shortening of the $\text{U}\cdots\text{OH}_2$ bond of the entering H_2O increases, while the bond lengths of the five spectator H_2O ligands are elongated slightly, which gives rise to a decrease of the BSSE. Thus the sum of these two BSSE contributions is approximately constant. For reaction (1), the BSSE was calculated at the HF level. The corresponding BSSE corrections for MCQDPT2 were obtained from the HF-BSSE by scaling ($\text{MCQDPT2-BSSE} = \text{HF-BSSE} \times 16.5/9.3$).

Electron correlation in dioxouranium(VI) complexes: In all of the investigated UO_2^{2+} ions, there is static electron correlation in addition to the omnipresent dynamic correlation. As found from the CI calculations (see Computational Methods), static correlation arises from the population of $\sigma^*(\text{O}=\text{U}=\text{O})$ and $\pi^*(\text{O}=\text{U}=\text{O})$ MOs by $\sigma(\text{O}=\text{U}=\text{O})$ and $\pi(\text{O}=\text{U}=\text{O})$ electrons (Figure 1) as in the $[\text{VO}(\text{OH}_2)_5]^{2+}$ ion.^[16] The $\sigma^*(\text{O}=\text{U}=\text{O})$ natural orbital, NO 45, exhibiting an occupation of <0.02 electrons (Figure 1c) was not taken into the active space of the CAS-SCF(12/11) calculations, because its inclusion did not affect the geometry significantly (see below), and because of its considerably lower NO occupation (Figure 1). This low population is considered to arise from dynamic correlation (which is taken into account by second-order perturbation theory). Table 3 summarizes the multiconfiguration self-consistent field energies (MCSCF(12/11)-PCM) of the hydrated $[\text{UO}_2(\text{OH}_2)_5]^{2+}$ ion (CAS-SCF(12/11)-PCM structure with $\sim C_{2v}$ symmetry, see next section). The active space was the same as for the CAS-SCF(12/11)-SCRF/PCM calculations, but the degree of electron excitation was varied. These computations were performed using the occupation-restricted multiple active space (ORMAS) method developed by Ivancic.^[41] The error (ΔE) with respect to the CAS-SCF(12/11)-PCM energy is large for an excitation degree of two electrons. This indicates that (single-reference) CI singles–doubles and MP2

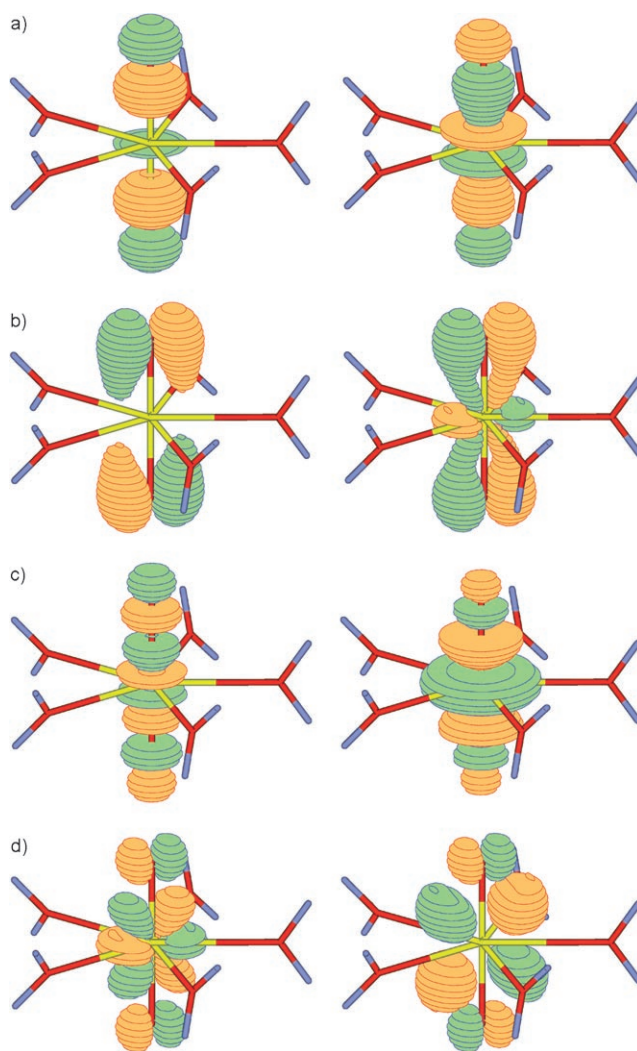


Figure 1. Natural orbitals (NOs) of the $[\text{UO}_2(\text{OH}_2)_5]^{2+}$ ion (CAS-SCF(12/12)-SCRF structure with D_5 symmetry): a) $\sigma(\text{O}=\text{U}=\text{O})$, NOs 36 and 37 with occupations of 1.9565 and 1.9530, respectively; b) two degenerate $\pi(\text{O}=\text{U}=\text{O})$ pairs, NOs 34/35 and 38/39 with occupations of 1.9602 and 1.9475, respectively; c) $\sigma^*(\text{O}=\text{U}=\text{O})$, NOs 40 and 45 with occupations of 0.0712 and 0.0196, respectively; d) two degenerate $\pi^*(\text{O}=\text{U}=\text{O})$ pairs, NOs 41/42 and 43/44 with occupations of 0.0559 and 0.0362, respectively.

Table 3. Dependence of the MCSCF(12/11)-PCM energy of $[\text{UO}_2(\text{OH}_2)_5]^{2+}$ on the number of excitable electrons.

Excitation level	Number of determinants	$E(\text{MCSCF}(12/11)\text{-PCM})$ [hartrees]	ΔE [kJ mol ⁻¹]
10 ^[a]	213 444	-580.623377	reference
8	212 508	-580.623375	0.0
6	172 683	-580.623342	0.1
4	45 311	-580.621554	4.8
2	1261	-580.597351	68.3

[a] This corresponds to the CAS-SCF(12/11)-PCM calculation.

techniques are not applicable. Another indication that MP2 is not suitable arises from the low contribution (87.6%) of the HF electron configuration in the CAS-SCF(12/11) wavefunction. For an excitation level of four, the error is much smaller, but not negligible. Hence, MP4(SDQ), for example,

might not be appropriate either. Agreement with the CAS-SCF(12/11)-PCM energy is obtained for excitations of six and eight electrons. A presently feasible treatment of electron correlation, which is expected to approach the full CI limit as closely as possible, involves the second-order perturbation calculation of the MCSCF(12/11) wavefunction with an excitation level of at least six. The MCQDPT2(12/11) method corresponds to such a computation with an excitation level of ten. The data in Table 3 show that quantum chemical methods that involve a total excitation degree below eight are unlikely to approach the full CI limit. Alternatively, coupled-cluster methods might also be suitable, but, for the present systems, they are much more demanding in terms of CPU time.

Geometry and its effect on the energy

$[\text{UO}_2(\text{OH}_2)_5]^{2+}$: All of the aqua complexes of UO_2^{2+} were investigated with CAS-SCF(12/11), because of the presence of static electron correlation, as described in the previous section. Accurate computations on aqueous UO_2^{2+} ions require CAS-SCF-based second-order perturbation theory, such as CASPT2,^[42,43] MCQDPT2^[22,23] or coupled-cluster^[21] methods, and an adequate treatment of hydration. Today, such techniques are applicable for the present energy computations, but not for the geometry optimizations. Hence, for the latter, approximations were unavoidable. Hydration was treated with the SCRf model (which includes monopole-dipole and dipole-dipole solute-solvent interactions)^[33-35] or PCM.^[6-8,37] For $[\text{UO}_2(\text{OH}_2)_5]^{2+}$ exhibiting D_5 symmetry and, therefore, no permanent electric dipole moment, the SCRf geometries are identical to those of the free ions (in the gas phase). The PCM geometries are considerably more computationally demanding, and are more accurate than those obtained with SCRf (Table 4).

DFT, in particular B3LYP, treats static and dynamic electron correlation adequately, since the U=O and U-O bond lengths agree with experiment (Table 4). The fact that the U-O bonds are still too long probably arises from the neglect of solvent to solute charge transfer (which is neglected

in both the SCRf and PCM calculations). Alternatively, the geometries were computed with CAS-SCF methods, in which dynamic electron correlation is neglected. The U=O bond lengths agree with experiment, but the U-O bonds are longer than with B3LYP, because of the neglect of dynamic correlation. The geometries are virtually equal for the (12/11) and the (12/12) active spaces. The $[\text{UO}_2(\text{OH}_2)_5]^{2+}$ ion has D_5 symmetry (Figure 2a), except for the CAS-SCF(12/

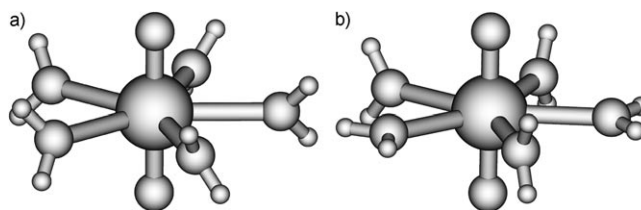


Figure 2. Perspective view of the $[\text{UO}_2(\text{OH}_2)_5]^{2+}$ ion: a) CAS-SCF(12/11)-SCRf structure with D_5 symmetry, and b) CAS-SCF(12/11)-PCM structure with $\sim C_{2v}$ symmetry.

11)-PCM computations, for which the symmetry is $\sim C_{2v}$ (Figure 2b). The CAS-SCF(12/11)-PCM species, calculated with $\sim D_5$ symmetry, exhibited three imaginary vibrational frequencies, which indicated that a more stable conformer exists. The U=O bond lengths obtained with HF are too short due to the neglect of static electron correlation.

For each geometry (Table 4), the energy was computed with the best available method, MCQDPT2(12/11)-PCM, which takes into account static and dynamic electron correlation as well as hydration with PCM. The energy of the CAS-SCF(12/11)-SCRf species is higher by $\approx 14 \text{ kJ mol}^{-1}$ than that of its corresponding PCM analog because of the longer U-O bonds. The HF-SCRf species has a considerably higher energy. The B3LYP-PCM structure has the lowest energy, since only with B3LYP is dynamic electron correlation taken into account in the geometry optimization.

$[\text{UO}_2(\text{OH}_2)_5 \cdots \text{OH}_2]^{2+}$ (Transition state for the A mechanism): This transition state (Figure 3) exhibits a weak U \cdots O

bond and two hydrogen bonds, which are absent in the $[\text{UO}_2(\text{OH}_2)_5]^{2+}$ ion (Figure 2). The errors in the U=O and U-O bond lengths are as in $[\text{UO}_2(\text{OH}_2)_5]^{2+}$, whereby BLYP gives less accurate results than B3LYP (Table 5). The U \cdots O bond length depends slightly on the computational method and the treatment of hydration, but it is not affected by p polarization functions added on the H atoms. In contrast, the two hydrogen bonds, H \cdots O, of the incoming (or leaving) H_2O with two H_2O molecules

Table 4. Bond parameters of the $[\text{UO}_2(\text{OH}_2)_5]^{2+}$ ion (exhibiting D_5 symmetry, unless noted otherwise), computed with various methods.^[a]

Method	$d(\text{U}=\text{O})$	$d(\text{U}-\text{O})$	$d(\text{O}-\text{H})$	$\angle(\text{HOH})$	$\angle(\text{H}_2\text{O}-\text{UO}_2)^{[b]}$	$\Delta E^{[c]}$
EXAFS ^[d]	1.76	2.41				
EXAFS ^[e]	1.77	2.42				
HF-SCRf	1.695	2.535	0.951	107.8	24.8	48.0
CAS-SCF(12/11)-SCRf	1.751	2.549	0.950	107.7	26.1	13.9
CAS-SCF(12/11)-SCRf ^[f]	1.750	2.555	0.949	106.7	24.0	
CAS-SCF(12/12)-SCRf	1.760	2.550	0.950	107.7	26.3	
B3LYP-PCM	1.77 ^[g]	2.46 ^[g]	0.97 ^[g]	107.9 ^[g]	~ 36 ^[g]	-10.9
CAS-SCF(12/11)-PCM	1.76 ^[g,h]	2.51 ^[g,h]	0.95 ^[g,h]	107.8, 108.6 ^[g,h]	$\sim 0, \sim 90$ ^[g,h]	0.0 ^[h]
CAS-SCF(12/11)-PCM	1.76 ^[g,i]	2.51 ^[g,i]	0.95 ^[g,i]	108.0 ^[g,i]	~ 34 ^[g,i]	3.7 ^[i]

[a] Units: bond lengths (d): Å, angles (\angle): °, energy differences (ΔE): kJ mol^{-1} . [b] Torsional angle between H_2O and the UO_2 fragment. [c] Calculated at the MCQDPT2(12/11)-PCM level. [d] Reference [44]. [e] Reference [45]. [f] 6-31G(d,p) basis set for H_2O . [g] Average values; the computation had to be performed in C_1 symmetry. [h] $[\text{UO}_2(\text{OH}_2)_5]^{2+}$ with $\sim C_{2v}$ symmetry. [i] $[\text{UO}_2(\text{OH}_2)_5]^{2+}$ with $\sim D_5$ symmetry, exhibiting three imaginary frequencies (168.7i, 103.5i, 61.4i cm^{-1}).

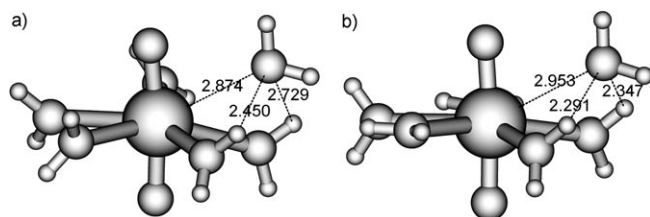
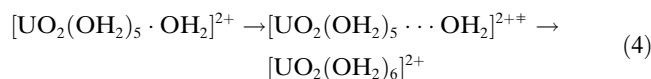
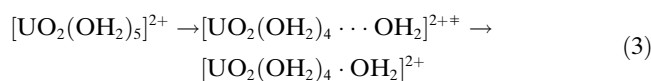


Figure 3. Perspective view of the transition state $[\text{UO}_2(\text{OH}_2)_5 \cdots \text{OH}_2]^{2+}$ for the A mechanism: a) CAS-SCF(12/11)-SCRF, and b) CAS-SCF(12/11)-PCM geometries.

in the first coordination sphere (Figure 3) are very sensitive to the quantum chemical method: the two hydrogen-bond lengths calculated with the ab initio MO methods HF or CAS-SCF differ greatly from those obtained with DFT methods, such as B3LYP and BLYP. Furthermore, they also depend on the treatment of hydration. The polarization functions on the H atoms cause an elongation of one hydrogen bond (by $\approx 0.07 \text{ \AA}$); otherwise their influence on the geometries is weak. The present results are in line with previous findings on aqua ions,^[16] that the currently used functionals might yield inaccurate and, in some cases, even unreliable hydrogen bonds. Furthermore, weak metal–ligand and hydrogen bonds in transition states, for example, might not be balanced correctly.^[16] Because of these rather severe limitations of B3LYP (and BLYP), already mentioned in the Introduction section, DFT was not used for the investigation of reaction (1), even though B3LYP yields more accurate U–O bond lengths. The conformation of the equatorial H_2O ligands (Figure 3) depends on the treatment of hydration. For SCRf and PCM solvation, they differ in a similar way as in $[\text{UO}_2(\text{OH}_2)_5]^{2+}$.

For each geometry (Table 5), the energy was computed at the MCQDPT2(12/11)-PCM level as for $[\text{UO}_2(\text{OH}_2)_5]^{2+}$. The deviations with respect to the CAS-SCF(12/11)-PCM geometry resemble those of $[\text{UO}_2(\text{OH}_2)_5]^{2+}$. The energy difference of the B3LYP-PCM geometry of $[\text{UO}_2(\text{OH}_2)_5 \cdots \text{OH}_2]^{2+}$ is slightly larger than that of $[\text{UO}_2(\text{OH}_2)_5]^{2+}$, despite the inaccuracy of the hydrogen bonds. At least for the present two ions, $[\text{UO}_2(\text{OH}_2)_5]^{2+}$ and $[\text{UO}_2(\text{OH}_2)_5 \cdots \text{OH}_2]^{2+}$, the energy errors arising from inaccurate geometries are approximately constant and tend to cancel out (Tables 4 and 5). However, the errors arising from inadequate methods for the energy computation, in particular B3LYP and BLYP, do not cancel (Table 1).

Mechanism of the water-exchange reaction of $[\text{UO}_2(\text{OH}_2)_5]^{2+}$: The D [Eq. (3)] and the A [Eq. (4)] mechanisms^[17,46] of reaction (1) were investigated on the basis of the previously introduced model.^[3,4]



The geometries of the reactants ($[\text{UO}_2(\text{OH}_2)_5]^{2+}$ and $[\text{UO}_2(\text{OH}_2)_5 \cdot \text{OH}_2]^{2+}$), the transition states ($[\text{UO}_2(\text{OH}_2)_4 \cdots \text{OH}_2]^{2+\ddagger}$ and $[\text{UO}_2(\text{OH}_2)_5 \cdots \text{OH}_2]^{2+\ddagger}$), and the hexacoordinated ($[\text{UO}_2(\text{OH}_2)_4 \cdot \text{OH}_2]^{2+}$) and octacoordinated ($[\text{UO}_2(\text{OH}_2)_6]^{2+}$) intermediates were optimized with CAS-SCF(12/11), for which hydration was treated with the computationally efficient SCRf model and the superior, but computationally rather demanding PCM. The Hessians were computed with the same method as the geometries, CAS-SCF(12/11)-SCRf or CAS-SCF(12/11)-PCM. Unscaled vibrational frequencies were used for the calculation of the zero-point energy (ZPE) and the thermodynamic variables. The total energies (E) were computed at the MCQDPT2(12/11)-PCM level. ΔE^\ddagger is the activation energy without ZPE and thermal corrections. The activation enthalpy (ΔH^\ddagger) was based on ΔE^\ddagger , to which the ZPE and the corresponding thermal corrections were added (see Computational Methods). The activation free enthalpy (ΔG^\ddagger) includes the activation entropy (ΔS^\ddagger). ΔE , ΔH , ΔG , and ΔS represent the corresponding variables for the intermediates. All of the thermodynamic data was computed for 25 °C.

The CAS-SCF(12/11)-SCRf structures (Figures 2a, 3a, S1, and S2) are similar to those found by Vallet et al.^[5] at the HF-CPCM level, but the CAS-SCF(12/11)-PCM structures of $[\text{UO}_2(\text{OH}_2)_5]^{2+}$, $[\text{UO}_2(\text{OH}_2)_5 \cdots \text{OH}_2]^{2+\ddagger}$, and $[\text{UO}_2(\text{OH}_2)_4]^{2+}$ exhibit different conformations of the H_2O ligands. As already mentioned, the SCRf structure of $[\text{UO}_2(\text{OH}_2)_5]^{2+}$ has D_5 symmetry at the CAS-SCF(12/11)-SCRf level, whereas the symmetry of the corresponding PCM structure is $\sim C_{2v}$ (Figure 2). The energy difference (ΔE) between these two conformers is small (Table 4), but not so the entropy difference (see below). For $[\text{UO}_2(\text{OH}_2)_5]^{2+}$, Bühl et al.^[10a] also obtained two structures with close energies, one being the species with D_5 symmetry. All of the at-

Table 5. Selected bond lengths of the transition state $[\text{UO}_2(\text{OH}_2)_5 \cdots \text{OH}_2]^{2+\ddagger}$ for the A Mechanism.^[a]

Method	$d(\text{U}=\text{O})$	$d(\text{U}-\text{O})$	$d(\text{U} \cdots \text{O})$	$d(\text{H} \cdots \text{O})$	$\Delta E^{[b]}$
HF-SCRf	1.697, 1.696	2.531, 2.550, 2.551, 2.547, 2.632	2.887	2.442, 2.698	50.6
CAS-SCF(12/11)-SCRf	1.752, 1.753	2.549, 2.566, 2.569, 2.563, 2.662	2.874	2.450, 2.729	16.2
CAS-SCF(12/11)-SCRf ^[c]	1.751, 1.751	2.572, 2.570, 2.573, 2.560, 2.680	2.864	2.524, 2.734	
B3LYP-SCRf	1.764, 1.762	2.472, 2.507, 2.498, 2.552, 2.554	2.961	1.951, 3.031	-1.1
BLYP-SCRf	1.806, 1.805	2.489, 2.517, 2.511, 2.543, 2.585	2.986	1.913, 3.203	2.8
CAS-SCF(12/11)-PCM	1.759, 1.760	2.529, 2.569, 2.533, 2.532, 2.533	2.953	2.291, 2.347	0.0
B3LYP-PCM	1.771, 1.770	2.466, 2.496, 2.466, 2.504, 2.501	2.975	1.858, 2.597	-14.2

[a] Units: bond lengths (d): Å, energy differences (ΔE): kJ mol^{-1} . [b] Calculated at the MCQDPT2(12/11)-PCM level. [c] 6-31G(d,p) basis set for H_2O .

tempts to compute a CAS-SCF(12/11)-SCRf structure like the PCM one failed. With SCRf and PCM hydration, the same conformation of the H₂O ligands in the transition state for the D mechanism, [UO₂(OH₂)₅⋯OH₂]^{2+‡}, was found (Figure S1); attempts at calculating a species with two H₂O ligands perpendicular to each other, as in [UO₂(OH₂)₅]²⁺ with ~C_{2v} symmetry, failed. The conformation of the H₂O ligands in the transition state and the intermediate for the A mechanism are as in the reactant [UO₂(OH₂)₅]²⁺. For both pathways, the transition states obtained with PCM hydration have a higher symmetry than those with SCRf.

Experimental and computed activation parameters for reaction (1), proceeding by means of the D and the A mechanisms, are summarized in Table 6. The present CAS-SCF(12/11)-SCRf/PCM ΔE[‡] and ΔE (Table 6) are compared with those of Vallet et al.^[5] (Table 6). For the D pathway, their ΔE[‡] (not corrected for the BSSE) is *higher* by 6.6–9.6 kJ mol⁻¹ than the present data (also without BSSE corrections), whereas for the A mechanism, it is *lower* by 9.2–12.6 kJ mol⁻¹. Their ΔE[‡] favors the A mechanism by ≈40 kJ mol⁻¹ in contrast to the present results, according to which A is considerably less favored, by 18.8–21.7 kJ mol⁻¹. ΔE follows similar trends. Upon inclusion of BSSE corrections (Table 6), ΔE[‡] (as well as ΔH[‡] and ΔG[‡]) increases for both mechanisms by ≈3–4 kJ mol⁻¹, whereas the A–D ΔE[‡], ΔH[‡], and ΔG[‡] differences remain virtually unchanged. Furthermore, the A–D energy difference is not affected by additional p polarization functions on the H₂O ligands (Table 6).

Before discussing the computed ΔH[‡], ΔS[‡] and ΔG[‡] values, an observation of Cooper and Ziegler^[47] is presented. In a study on substitution reactions on square planer Pd²⁺

complexes with H₂O, NH₃, and Cl⁻ ligands, they found that ΔG[‡] agrees with experiment in contrast to ΔH[‡] and ΔS[‡], because of a compensation of errors. These errors arise from the model in which specific solute–solvent interactions, and solvent–solvent interactions in proximity of the solute, that might differ from those in the bulk, are neglected.

In PCM^[6–8] calculations, the electrostatic component of the solute–solvent interactions is taken into account, but solvent to solute charge transfer is neglected as well as the directionality of the hydrogen bonds. These simplifications give rise to some (computed) vibrational frequencies of coordinated water molecules that are too low. For [Fe(OH₂)₆]²⁺ and [Co(OH₂)₆]²⁺, exhibiting water-exchange rates of the same order of magnitude as [UO₂(OH₂)₅]²⁺, librational modes (R_x, R_y, R_z) of 597, 675, 418 and 623, 564, 382 cm⁻¹, respectively, have been obtained by Rode and co-workers.^[48,49] For each of the presently investigated UO₂²⁺ species, there are up to ten vibrational modes exhibiting frequencies much too low, with values below 150 cm⁻¹. In the course of the exchange reactions [Eqs. (3) and (4)], some of these low-frequency modes change considerably. Thus, the accuracy of the vibrational partition functions is unknown; their error might be sizable. ΔS and ΔS[‡] are expected to be affected most strongly, whereas, as pointed out by Cooper and Ziegler,^[47] this error might cancel approximately for ΔG and ΔG[‡]. As an artifact of the present model, including only the first coordination sphere and a single H₂O in the second sphere [Eqs. (3) and (4)], the conformations of the H₂O molecules depend on the method for the treatment of hydration. It will be shown in the following, that mainly ΔS and ΔS[‡] are affected by the differing H₂O conformations, which arise from the geometry optimizations on the basis of SCRf or PCM hydration.

Table 6. Experimental and computed thermodynamic activation parameters.^[a]

Mechanism	ΔE [‡] (ΔE)	ΔH [‡] (ΔH)	ΔS [‡] (ΔS)	ΔG [‡] (ΔG)	ΔV _{cav} [‡] (ΔV _{cav})
experimental data ^[b]		26	-40	38	
CAS-SCF(12/11)-SCRf geometries/frequencies, and MCQDPT2(12/11)-PCM energies ^[c,d]					
D	50.1 (44.3)	48.4 (46.2)	2.7 (11.4)	47.6 (42.8)	6.9 (8.7)
D	49.6 (45.2 ^[e])	48.2 ^[e] (47.3 ^[e])	-0.3 ^[e] (8.3 ^[e])	48.3 ^[e] (44.9 ^[e])	6.3 ^[e] (8.2 ^[e])
A	31.3 (29.5)	27.2 (27.7)	-17.7 (-0.4)	32.4 (27.8)	-4.1 (-3.6)
A	27.9 (26.9 ^[e])	23.6 ^[e] (25.0 ^[e])	-11.6 ^[e] (7.7 ^[e])	27.0 ^[e] (22.7 ^[e])	-3.9 ^[e] (-3.7 ^[e])
CAS-SCF(12/11)-PCM geometries/frequencies, and MCQDPT2(12/11)-PCM energies ^[c,d]					
D	52.6 (47.9)	50.0 (48.7)	-24.0 (-14.9)	57.1 (53.2)	3.1 (3.6)
D	55.3 ^[f] (48.4 ^[f])	52.7 ^[f] (49.2 ^[f])		59.8 ^[f] (53.7 ^[f])	
A	31.0 (26.0)	28.4 (25.7)	-23.4 (-2.4)	35.3 (26.4)	-2.4 (-2.9)
A	35.0 ^[f] (30.9 ^[f])	32.4 ^[f] (30.6 ^[f])		39.3 ^[f] (31.3 ^[f])	
HF-CPCM geometries/MP2-CPCM energies ^[c,g]					
D	59.2 (54.5)	[h]	[h]	[h]	4.9 (3.6)
A	18.7 (15.8)	[h]	[h]	[h]	-3.0 (-3.4)
CPMD geometries/CPMD energies ^[c,i]					
D				45.2 (36.4) ^[j]	
A				28.0 (26.8) ^[j]	

[a] Units: energies: kJ mol⁻¹, entropy: JK⁻¹mol⁻¹, volume: cm³mol⁻¹. [b] From reference [1]. [c] In parentheses: parameters for the corresponding intermediate. [d] This work. [e] 6–31G(d,p) basis set for H₂O. [f] Corrected for the BSSE. [g] From reference [5]. [h] The vibrational frequencies were not computed. [i] From reference [10] [j] ΔA[‡] (ΔA), Helmholtz free energy at 27 °C.

The deviation in ΔS[‡] is sizable (Table 6), because of the above-mentioned limitations in the model. The computed ΔS[‡] values for the D mechanism appear to depend strongly on the treatment of hydration. An inspection of the entropy of [UO₂(OH₂)₅]²⁺ shows, however, that the PCM entropy (based on the ~C_{2v} species) is greater than the SCRf entropy by ≈25 JK⁻¹mol⁻¹. A small part of the difference in ΔS[‡] (for the D mechanism) arises from the different models for the treatment of hydration, and is due in large part to the different conformations of the H₂O ligands in the reactant [UO₂(OH₂)₅]²⁺ (Figure 2), since the SCRf and PCM entropies of the transition state [UO₂(OH₂)₄⋯OH₂]^{2+‡} (exhib-

iting the same conformation of the H₂O ligands) differ merely by $\approx 8 \text{ JK}^{-1} \text{ mol}^{-1}$. In the two conformers of $[\text{UO}_2(\text{OH}_2)_5]^{2+}$, the torsional frequencies of the H₂O ligands differ, since in the species with $\sim C_{2v}$ symmetry, there are four H \cdots O bonds within the coordinated H₂O molecules, which are shorter by $\approx 0.2 \text{ \AA}$ than in the D₅ structure. This example shows that the computed entropy might depend critically on the model. As a consequence, ΔG^\ddagger , depending on ΔS^\ddagger ($\Delta G^\ddagger = \Delta H^\ddagger - T\Delta S^\ddagger$), will also be affected by ΔS^\ddagger in cases, like the present one, in which ΔH^\ddagger (but not ΔS^\ddagger) is insensitive to the conformation of the ligands. For the D mechanism, the difference in ΔG^\ddagger based on SCRf and PCM hydration amounts to $\approx 10 \text{ kJ mol}^{-1}$.

Both methods for the treatment of hydration give rise to the same conformers of the reactant ($[\text{UO}_2(\text{OH}_2)_5 \cdot \text{OH}_2]^{2+}$) for the A mechanism (Figure S2). The conformation of the H₂O ligands in the transition state (Figure 3) and the intermediate differ as in $[\text{UO}_2(\text{OH}_2)_5]^{2+}$ (Figure 2). In this case, the different conformations do not give rise to substantially different ΔS^\ddagger values. All of the PCM conformers were obtained starting from the corresponding SCRf species. Attempts at obtaining other conformers with either SCRf or PCM hydration failed. The original CAS-SCF(12/11)-SCRf structure of $[\text{UO}_2(\text{OH}_2)_5]^{2+}$ was recovered when the computation was started from the corresponding CAS-SCF(12/11)-PCM geometry. The different conformers are due to differences in the PCM and SCRf models: in the more elaborate PCM, a shape-adapted cavity is used, and electrostatic solute–solvent interactions are taken into account.^[6–8] Since solute–solvent hydrogen bonding is mainly electrostatic, PCM is expected to describe the major influence of the second coordination sphere on the first sphere.

On the basis of both the CAS-SCF(12/11)-PCM and the CAS-SCF(12/11)-SCRf geometries, the D mechanism is less favorable than A by ≈ 20 – 22 and ≈ 15 – 21 kJ mol^{-1} , respectively. Furthermore, ΔG^\ddagger for the A mechanism is close to the experimental value, which suggests that this is the preferred water-exchange mechanism for reaction (1). The agreement of the computed ΔH^\ddagger with experiment lends additional support for the A mechanism; ΔH^\ddagger for D is higher by $\geq 20 \text{ kJ mol}^{-1}$.

The (BLYP-based) CPMD free activation energies of Bühl et al.^[10] for the D and A mechanisms (Table 6) are lower than the corresponding ΔG^\ddagger values. These deviations with respect to MCQDPT2 are smaller than those reported for transition metal aqua ions^[16] and the corresponding MCQDPT2-BLYP differences in Table 1.

The substitution mechanism can be derived from the activation volume (ΔV^\ddagger) or, more precisely, from its intrinsic component ($\Delta V_{\text{int}}^\ddagger$).^[46] The difference in solute cavity volume ($\Delta V_{\text{cav}}^\ddagger$) is approximately equal to $\Delta V_{\text{int}}^\ddagger$. These data, together with the reaction volumes for the formation of the intermediates (ΔV_{cav}), are included in Table 6. The absolute $\Delta V_{\text{cav}}^\ddagger$ values for both the A and the D pathways are larger for the SCRf geometries. The corresponding HF-CPCM data of Vallet et al.^[5] lies between the CAS-SCF(12/11)-SCRf and the CAS-SCF(12/11)-PCM values.

Lifetime of the intermediates: The lifetime of an intermediate (τ_1) may be calculated on the basis of the rate constant (k_1) with which it decays [Eq. (5)].^[4] k_1 is obtained from transition state theory [Eqs. (6)–(8)],^[50–52] in which k_B is the Boltzmann constant, h is Planck's constant, and R is the gas constant. ΔG_1^\ddagger [Eq. (7)] represents the free enthalpy difference (at 25 °C) between the intermediate and the corresponding transition state.

$$\tau_1 = 1/k_1 \quad (5)$$

$$k_1 = \Gamma_n \kappa \frac{k_B T}{h} e^{-\Delta G_1^\ddagger / RT} \quad (6)$$

$$\Delta G_1^\ddagger = \Delta G^\ddagger - \Delta G \quad (7)$$

$$\Gamma_n = 1 + \frac{1}{24} \left(\frac{h\nu^\ddagger}{k_B T} \right)^2 \quad (8)$$

The transition probability (κ) is assumed to be 1, and the nuclear tunneling factor (Γ_n), estimated on the basis of Wigner's equation [Eq. (8)],^[52] is close to 1, that is, 1.001–1.006 for the present reactions (ν^\ddagger is the imaginary frequency, being in the range of 39i–79i cm^{-1} for the present transition states). The lifetime (τ_1) of an intermediate may be shorter or of the order of the duration of the vibrational mode with which the intermediate reacts to form the product. In this case, the lifetime of an intermediate with an increased coordination number, for example $[\text{UO}_2(\text{OH}_2)_6]^{2+}$, could not be measured even if adequate experimental techniques existed, because it would decompose immediately after its formation. Experimentally, such an intermediate could not be distinguished from a transition state (because the “first” U–O stretching vibration would transform it into the product). Likewise, an intermediate with a reduced coordination number, for example $[\text{UO}_2(\text{OH}_2)_4 \cdot \text{OH}_2]^{2+}$, would react immediately with a molecule or ion in its second coordination sphere. No equilibration of the second coordination sphere with the bulk solution would be possible after the formation of the intermediate, since, as soon as the intermediate was formed, it would react immediately with a species in the second sphere to form the product.

For the present intermediates $[\text{UO}_2(\text{OH}_2)_4 \cdot \text{OH}_2]^{2+}$ and $[\text{UO}_2(\text{OH}_2)_6]^{2+}$ (Table 7), the duration (τ_{vib}) of the vibrational mode ($\tilde{\nu}$) leading to the product is 0.3–0.4 ps. τ_1 is approximately 1 ps, 2–3 times longer than τ_{vib} apart from the exception of the intermediate $[\text{UO}_2(\text{OH}_2)_6]^{2+}$ for the A mechanism, computed at the CAS-SCF(12/11)-PCM level, for which τ_1 is considerably longer than τ_{vib} . This species could be considered as a genuine intermediate.

Discussion

Electron correlation in dioxouranium(VI) complexes: Static electron correlation, which was shown to be present in the UO_2^{2+} fragment, can be treated with MCSCF involving an excitation level ≥ 6 . Thus, the treatment of static and dy-

Table 7. Properties of the intermediates $[\text{UO}_2(\text{OH}_2)_4]^{2+}$ and $[\text{UO}_2(\text{OH}_2)_6]^{2+}$ related to their lifetimes.

Mechanism	Geometry and frequency	ΔG^\ddagger [kJ mol ⁻¹] [Eq. (7)]	τ_1 [ps] [Eqs. (5)–(8)]	$\tilde{\nu}^{[a]}$ [cm ⁻¹]	$\tau_{\text{vib}}^{[b]}$ [ps]
D	CAS-SCF(12/11)-SCRF	4.8	1.1	98.4	0.34
D	CAS-SCF(12/11)-SCRF ^[c]	3.4	0.63	96.1	0.35
D	CAS-SCF(12/11)-PCM	3.9	0.8	94.7	0.35
D	CAS-SCF(12/11)-PCM	6.1 ^[d]	1.9 ^[d]		
A	CAS-SCF(12/11)-SCRF	4.6	1.0	81.9	0.41
A	CAS-SCF(12/11)-SCRF ^[c]	4.3	0.9	82.2	0.41
A	CAS-SCF(12/11)-PCM	8.9	5.8	100.6	0.33
A	CAS-SCF(12/11)-PCM	8.0 ^[d]	4.1 ^[d]		

[a] Vibrational mode giving rise to product formation. [b] Duration of the vibrational mode $\tilde{\nu}$, $\tau_{\text{vib}} = (c\tilde{\nu})^{-1}$ (c : speed of light). [c] 6–31G(d,p) basis set for the H₂O ligands. [d] Corrected for the BSSE.

dynamic electron correlation of aqua complexes of UO_2^{2+} requires a total excitation level of at least 8. MCQDPT2(12/11) as well as coupled-cluster methods satisfy this requirement. As can be seen in the three examples in Table 1, the MP2 energies are equal to those of MCQDPT2(12/11) and CCSD(T) in spite of an insufficient excitation level of only 2. Evidently, for the energies, but not the geometries^[39] (see Dependence of Activation and Reaction Energies on the Computational Method), there must be a compensation of errors, which is most likely to arise from the virtually constant U=O bond lengths of the UO_2^{2+} species involved in the water-exchange reactions by both the associative and the dissociative mechanisms.

Approximations in the present calculations: In the present study, the best level for the geometry and frequency computations is achieved with CAS-SCF(12/11)-PCM (Table 6). The ΔH^\ddagger and ΔG^\ddagger values for the A mechanism agree with experiment within 3 kJ mol⁻¹, whereas the corresponding data for the D mechanism is higher by ≈ 20 kJ mol⁻¹. This A–D energy difference is not altered upon addition of p polarization functions on the H atoms or BSSE corrections. Therefore, the dissociative mechanism is unlikely to operate for reaction (1). The computations are more accurate than the previous^[1,5,10] ones, because of an improved treatment of electron correlation. The agreement with experiment of the ΔH^\ddagger and ΔG^\ddagger energies computed for the A mechanism might suggest, erroneously, that the CAS-SCF(12/11)-PCM/MCQDPT2(12/11)-PCM calculations on the basis of the cluster model, represented by Equation (4), produce accurate thermodynamic activation parameters. It should be noted that, in spite of the demanding level of these calculations, a variety of approximations had to be made, giving rise to errors that are either negligible or which cancel largely:

- 1) Possible errors arising from the “split-valence + polarization” basis set cannot be assessed, since today, CAS-SCF(12/11)-PCM/MCQDPT2(12/11)-PCM computations with larger basis sets are very demanding.
- 2) Dynamic electron correlation was neglected in the geometry optimizations.
- 3) Charge transfer from the solvent to the solute dication as well as the covalent character of the solute–solvent hydrogen bonds are not treated with PCM.

- 4) The geometry was optimized by minimization of the quantum chemical total energy (E) and not the free enthalpy (G).
- 5) The accuracy of the vibrational partition functions is unknown.
- 6) The computed data depend on the conformation of the H₂O ligands.

Items 2) and 3) give rise to longer U–O bonds, and most likely also to errors in the entropies, but their effect on the energy differences is unknown. The consequences of approximation 4) are also unknown, and those of 5) and 6) have been discussed. The correction of item 2) is not (yet) feasible with ab initio methods, but it might be or become possible with DFT, if one of the currently developed functionals treats hydrogen bonding and weak metal–ligand bonds properly. The improvement of approximations 3), 5) and probably also 6) would require demanding CAS-SCF(12/11) computations with a quantum chemically described second hydration sphere (whereby items 5) and 6) alone might already be improved with a classical second sphere). Methods for the geometry optimization based on the free energy have been reported recently.^[53,54] These techniques are applicable for HF and DFT, but not yet for CAS-SCF.

Alternatively, hydration can be treated with molecular dynamics (MD) simulations. Very recently, such a study,^[55] in which the force field was derived from CASPT2(12/12) computations including corrections for the basis set superposition error, was published. The inclusion of an attractive term describing solvent water to uranyl(VI) charge transfer was necessary. No hydrogen bonding of (solvent) water with the oxo ligands was observed. All of the monitored events corresponded to the associative (A) pathway or “something between A and I”. Since during the short simulation time of 100 ps two water replacements were observed, the water-exchange rate was overestimated by several orders of magnitude (the experimental rate constant is $1.3 \times 10^6 \text{ s}^{-1}$ [1]). In another classical MD investigation based on nonrigid water molecules, the deprotonation of $[\text{UO}_2(\text{OH}_2)_5]^{2+}$ was investigated.^[56] Unconstrained ab initio MD (AIMD) simulations on reactions like the present one are prohibitive because of their long simulation times. However, activation free energies (ΔA^\ddagger) for the aquation of $[\text{cis-Pt}(\text{NH}_3)_2\text{Cl}_2]^{[57]}$ and the water-exchange reaction of $[\text{UO}_2(\text{OH}_2)_5]^{2+}$ ^[10] have been obtained with constrained AIMD. As already seen, ΔA^\ddagger for both the associative and the dissociative mechanisms are underestimated (Table 6). Furthermore, the choice and application of the constrained coordinate for the A mechanism was not straightforward.^[10b] Hydration can also be treated with hybrid quantum-mechanical/molecular-mechanical (QM/MM) methods, which have been used for the study of very fast exchange reactions, for example that of the aqua

ion of Ag^+ .^[58] Often, in ab initio or QM/MM MD simulations, exchange events cannot be observed within the available simulation time, even if the reaction rates are very high ($\geq 10^9 \text{ s}^{-1}$). In the absence of exchange events, the activation free energy (ΔA^\ddagger)^[59] or the mean residence time^[60,61] of water in the first coordination sphere can nevertheless be determined. On the basis of ΔA^\ddagger , the water-exchange rates of Na^+ , K^+ , Cs^+ , Ca^{2+} , Cu^{2+} , Ag^+ , Hg^{2+} , and Au^+ were obtained.^[62] The mean residence time of water in the first coordination sphere of Cs^+ , Ag^+ , Au^+ , Ca^{2+} , and Hg^{2+} were computed on the basis of Impey et al.^[60] as well as the direct^[61] method. The water-exchange rate of $[\text{Cu}(\text{OH}_2)_6]^{2+}$, the coordination number of which is debated,^[63] was investigated^[64] with QM/MM and the method of Impey et al.,^[60] in which the first and second coordination spheres were treated with HF. The computed mean residence time (of 21–23 ps) agrees with experiment. The water-exchange rates of ammine–aqua complexes of Ni^{2+} were found to proceed by means of the D mechanism, but the rates were overestimated by a factor of $\approx 10^4$.^[65]

For many systems, an associative as well as a dissociative pathway is feasible.^[17] For the understanding of the role of the ligands and the electronic structure of the metal ion on the reactivity, the energy difference between the associative and the dissociative mechanisms needs to be computed, if they both exist. In such cases, the computational method should not favor one pathway over the other. This requires that electron correlation and solvation are treated adequately. This has been achieved with the present computations and the constrained CPMD studies^[10] on reaction (1). Both methods produced the same ordering of ΔG^\ddagger or ΔA^\ddagger for the A and D mechanisms and favor the A pathway by similar energies, for which, as already mentioned, CPMD tends to underestimate the ΔA^\ddagger values for both pathways. Constrained QM/MM calculations at the CAS-SCF level would be an alternative, which has not been realized thus far.

Water-exchange mechanism of uranyl(VI) complexes: For $[\text{UO}_2(\text{OH}_2)_5]^{2+}$, the computed thermodynamic activation parameters (Table 6) favor the associative water-exchange pathway over the dissociative pathway on the basis of the lower ΔG^\ddagger and its agreement with experiment. ΔG^\ddagger for D depends on the conformation of the H_2O ligands in the reactant. The deviation of ΔG^\ddagger from the experimental value is not so large that this mechanism could be excluded with absolute certainty because of the approximations 1)–6), as discussed above.

Due to the very short lifetime (Table 7) of the intermediate $[\text{UO}_2(\text{OH}_2)_4\text{OH}_2]^{2+}$ (τ_1), which is only around three times longer than the duration of the vibration leading to the product (τ_{vib}), it might be more appropriate to attribute the I_d mechanism to the dissociative pathway, provided that it would nevertheless be more favorable than the associative mechanism. The corresponding ΔA_1^\ddagger ($=\Delta A^\ddagger - \Delta A$) value of 8.8 kJ mol^{-1} from the CPMD study^[10a] is larger than ΔG_1^\ddagger , again because of the preference of DFT for the species with a lower coordination number (the intermediate has a lower

coordination number than the transition state, since the latter exhibits an additional weak or partial $\text{U}\cdots\text{O}$ bond).^[16] Based on this value, $\tau_1 \approx 5.6 \text{ ps}$ is estimated, which would suggest the D instead of the I_d mechanism.

For the associative mechanism, the two methods for the treatment of hydration, yielding different conformations of the H_2O ligands in the transition state $[\text{UO}_2(\text{OH}_2)_5\cdots\text{OH}_2]^{2+}$ (Figure 3) and the intermediate $[\text{UO}_2(\text{OH}_2)_6]^{2+}$ (Figure S2), have a small effect on ΔE^\ddagger and ΔH^\ddagger , as well as ΔH and ΔG . ΔG_1^\ddagger differs by 4.3 kJ mol^{-1} for the two sets of computations, and although this is a modest difference, it is responsible for the difference of τ_1 by a factor of ≈ 6 (Table 7). Hence, the I_a mechanism would be attributed on the basis of the CAS-SCF(12/11)-SCRF geometries and frequencies. According to the CAS-SCF(12/11)-PCM computations, however, the reaction would proceed by the A mechanism because τ_1 is 12–18 times longer than the duration of the vibration (τ_{vib}) giving rise to product formation. The attributed mechanism depends critically on ΔG_1^\ddagger . The difference in the ΔG_1^\ddagger values based on SCRF or PCM geometries does not arise from the variation of the $T(\Delta S^\ddagger - \Delta S)$ terms (which amounts to 1.1 kJ mol^{-1}), but it is due to the ΔE_1^\ddagger ($=\Delta E^\ddagger - \Delta E$) terms which differ by 3.2 kJ mol^{-1} (for the SCRF and the PCM calculations). This is an example showing that small deviations, lying well within the error of the calculations, can have a determining influence on the conclusions. For the associative pathway, there might be some preference for the A mechanism on the basis of the intrinsically more accurate CAS-SCF(12/11)-PCM geometries and frequencies, although the I_a mechanism cannot be ruled out. If τ_1 is estimated from ΔE_1^\ddagger instead of ΔG_1^\ddagger , the I_a mechanism would be attributed on the basis of both methods for the treatment of hydration. It remains an open question, whether the present model [Eqs. (3) and (4)] and computational techniques can produce sufficiently accurate ΔG_1^\ddagger and τ_1 values, which could allow the distinction of the stepwise from the concerted mechanism. The intermediates of both mechanisms have very short lifetimes, being of the order of picoseconds. Longer lifetimes, in the nano- or microsecond regime, are unlikely.

In their second CPMD study, Bühl and Kabrede^[10b] claimed that the I_a mechanism operates for reaction (1) on the basis of the small ΔA_1^\ddagger value of $\approx 1.2 \text{ kJ mol}^{-1}$. For the energies, they estimated an error of $\approx 4.2 \text{ kJ mol}^{-1}$, which suggests that their ΔA_1^\ddagger value is rather inaccurate. Furthermore, as shown in the Results section (Lifetime of the Intermediates), it is not on the basis of the magnitude of ΔG_1^\ddagger (or ΔA_1^\ddagger) alone, but on the basis of the ratio of τ_1/τ_{vib} [Eqs. (5)–(8), Table 7] that stepwise mechanisms can be distinguished from concerted ones. Bühl and Kabrede's data certainly does not allow the definitive assignment of the I_a mechanism.

The present discussion shows that the distinction of the stepwise (D or A) from the concerted (I_d or I_a) mechanism has to be made on the basis of small energy differences (ΔG_1^\ddagger) the errors of which, although small, can be critical. It is not my intention to make definitive statements as to whether the stepwise or the concerted pathway operates, but to supply criteria which are based on physical quantities.

In an earlier study^[66] on the water-exchange reaction of $[\text{CrL}_5\text{OH}_2]^{3+}$ complexes, the influence of the ligands which do not participate in the water-exchange process (the “spectator” ligands) on the mechanism was analyzed. For L ligands that are weak electron donors, such as H_2O , the associative character is most pronounced. The reaction proceeds by the I_a mechanism with the shortest $\text{Cr}\cdots\text{O}$ bonds in the transition state $[(\text{OH}_2)_5\text{Cr}\cdots(\text{OH}_2)_2]^{3+\ddagger}$. If the ligand *trans* to the exchanging H_2O is replaced by a stronger electron donor, such as NH_3 or NH_2CH_3 , the $\text{Cr}\cdots\text{O}$ bonds are longer. Replacement of the *cis* ligands by stronger donors has a weaker effect on the $\text{Cr}\cdots\text{O}$ bonds. The exchange mechanism becomes dissociative (D or I_d), when the five H_2O ligands are replaced by five NH_2CH_3 ligands. The replacement of the rather weak electron donor H_2O by stronger donors, more basic ligands, reduces the associative character of the mechanism or increases its dissociative character, for which the effect of the *trans* ligand is larger than that of *cis* ligands.

For the water-exchange reaction of $[\text{UO}_2(\text{OH}_2)_5]^{2+}$, an associative as well as a dissociative pathway is feasible, for which the associative mechanism is more advantageous by a modest free enthalpy difference of $\approx 15\text{--}21$ or $\approx 20\text{--}22$ kJ mol^{-1} for SCRF or PCM hydration (Table 6). In the present context, the question whether the reaction follows a stepwise (A or D) or a concerted (I_a or I_d) mechanism, is not relevant. The application of the principles based on the $[\text{CrL}_5\text{OH}_2]^{3+}$ study^[66] suggests that the replacement of some of the H_2O ligands of $[\text{UO}_2(\text{OH}_2)_5]^{2+}$ by stronger electron donors, for example F^- or $\text{C}_2\text{O}_4^{2-}$, is expected to lower the activation energy for the dissociative pathway and to raise that for the associative pathway.

The water-exchange reaction of $[\text{UO}_2(\text{C}_2\text{O}_4)_2\text{OH}_2^{2-}]$ was claimed^[5] to follow the A mechanism. The geometries were optimized at the HF level for the free ions in the gas phase, and the energy was computed at the CPCM-MP2 level.^[5] Because of the presence of permanent electric dipole moments in the pertinent oxalato complexes, the gas-phase geometries are questionable and furthermore, the $\text{U}=\text{O}$ bonds are too short (it should be noted that SCRF calculations are not more demanding than gas-phase calculations). Hence, the conclusion of Vallet et al.^[5] that this water-exchange reaction proceeds by means of the A mechanism is based on inappropriate computational techniques and furthermore, it contradicts the expected trends as discussed above, when four weak H_2O ligands are replaced by two bidentate and stronger $\text{C}_2\text{O}_4^{2-}$ donors. The data in Table 1 suggests that the HF energies are, possibly fortuitously, close to the MCQDPT2 and CCSD(T) values. It is interesting to note that the gas-phase HF data of Vallet et al.^[5] favor the D mechanism over A by ≈ 21 kJ mol^{-1} (“ $\Delta U(\text{SCF})$ ” column in Table 6 of reference [5]). This can be taken as a support for the expected dissociative pathway.

The water-exchange mechanism of $[\text{UO}_2\text{F}_4(\text{OH}_2)^{2-}]$, resembling $[\text{UO}_2(\text{C}_2\text{O}_4)_2\text{OH}_2^{2-}]$, was also investigated by Vallet et al.,^[15] who found, on the basis of their usual approximations (HF-CPCM geometries/MP2-CPCM energies),

that the D pathway is preferred over I, as expected for a system in which four H_2O ligands have been replaced by stronger F^- donors. Apart from one exception (deviating by ≈ 12 kJ mol^{-1}), the HF activation parameters are equal to those based on MP2.

The substitution mechanism of UO_2^{2+} complexes depends on their ligands: for weak electron donors (such as H_2O), the associative pathway is preferred if steric effects are absent. Complexes with stronger donors (for example OH^- , F^- or $\text{C}_2\text{O}_4^{2-}$) react preferentially through the dissociative pathway.

Acknowledgements

One reviewer contributed valuable comments on the manuscript.

- [1] I. Farkas, I. Bányai, Z. Szabó, U. Wahlgren, I. Grenthe, *Inorg. Chem.* **2000**, *39*, 799.
- [2] R. Åkesson, L. G. M. Pettersson, M. Sandström, U. Wahlgren, *J. Am. Chem. Soc.* **1994**, *116*, 8705.
- [3] F. P. Rotzinger, *J. Am. Chem. Soc.* **1996**, *118*, 6760.
- [4] F. P. Rotzinger, *J. Am. Chem. Soc.* **1997**, *119*, 5230.
- [5] V. Vallet, U. Wahlgren, B. Schimmelpfennig, Z. Szabó, I. Grenthe, *J. Am. Chem. Soc.* **2001**, *123*, 11999.
- [6] J. Tomasi, M. Persico, *Chem. Rev.* **1994**, *94*, 2027.
- [7] J. Tomasi, *Theor. Chem. Acc.* **2004**, *112*, 184.
- [8] J. Tomasi, B. Mennucci, R. Cammi, *Chem. Rev.* **2005**, *105*, 2999.
- [9] V. Barone, M. Cossi, *J. Phys. Chem. A* **1998**, *102*, 1995.
- [10] a) M. Bühl, R. Diss, G. Wipff, *J. Am. Chem. Soc.* **2005**, *127*, 13506; b) M. Bühl, H. Kabrede, *Inorg. Chem.* **2006**, *45*, 3834.
- [11] R. Car, M. Parrinello, *Phys. Rev. Lett.* **1985**, *55*, 2471.
- [12] A. D. Becke, *Phys. Rev. A* **1988**, *38*, 3098.
- [13] C. Lee, W. Yang, R. G. Parr, *Phys. Rev. B* **1988**, *37*, 785.
- [14] B. Miehl, A. Savin, H. Stoll, H. Preuss, *Chem. Phys. Lett.* **1989**, *157*, 200.
- [15] V. Vallet, U. Wahlgren, Z. Szabó, I. Grenthe, *Inorg. Chem.* **2002**, *41*, 5626.
- [16] F. P. Rotzinger, *J. Phys. Chem. B* **2005**, *109*, 1510.
- [17] F. P. Rotzinger, *Chem. Rev.* **2005**, *105*, 2003.
- [18] A. D. Becke, *J. Chem. Phys.* **1993**, *98*, 5648.
- [19] P. J. Stephens, F. J. Devlin, C. F. Chabrowski, M. J. Frisch, *J. Phys. Chem.* **1994**, *98*, 11623.
- [20] R. H. Hertwig, W. Koch, *Chem. Phys. Lett.* **1997**, *268*, 345.
- [21] P. Piecuch, S. A. Kucharski, K. Kowalski, M. Musial, *Comput. Phys. Commun.* **2002**, *149*, 71.
- [22] H. Nakano, *J. Chem. Phys.* **1993**, *99*, 7983.
- [23] H. Nakano, *Chem. Phys. Lett.* **1993**, *207*, 372.
- [24] M. W. Schmidt, K. K. Baldridge, J. A. Boatz, S. T. Elbert, M. S. Gordon, J. H. Jensen, S. Koseki, N. Matsunaga, K. A. Nguyen, S. J. Su, T. L. Windus, M. Dupuis, J. A. Montgomery, *J. Comput. Chem.* **1993**, *14*, 1347.
- [25] P. J. Hay, R. L. Martin, *J. Chem. Phys.* **1998**, *109*, 3875.
- [26] W. J. Hehre, R. Ditchfield, J. A. Pople, *J. Chem. Phys.* **1972**, *56*, 2257.
- [27] R. Ditchfield, W. J. Hehre, J. A. Pople, *J. Chem. Phys.* **1971**, *54*, 724.
- [28] A. Schäfer, H. Horn, R. Ahlrichs, *J. Chem. Phys.* **1992**, *97*, 2571.
- [29] G. Schaftenaar, J. H. Noordik, *J. Comput.-Aided Mol. Des.* **2000**, *14*, 123.
- [30] W. H. Miller, N. C. Handy, J. E. Adams, *J. Chem. Phys.* **1980**, *72*, 99.
- [31] N. Davidson, *Statistical Mechanics*, McGraw-Hill, New York, San Francisco, Toronto, London, **1962**, p. 105 (chapter 8).
- [32] C. F. Bender, E. R. Davidson, *J. Phys. Chem.* **1966**, *70*, 2675.
- [33] J. G. Kirkwood, *J. Chem. Phys.* **1934**, *2*, 351.
- [34] L. Onsager, *J. Am. Chem. Soc.* **1936**, *58*, 1486.

- [35] M. Szafran, M. M. Karelson, A. R. Katritzky, J. Koput, M. C. Zerner, *J. Comput. Chem.* **1993**, *14*, 371.
- [36] F. P. Rotzinger, *J. Phys. Chem. A* **1999**, *103*, 9345.
- [37] E. Cancès, B. Mennucci, J. Tomasi, *J. Chem. Phys.* **1997**, *107*, 3032.
- [38] P. J. Hay, R. L. Martin, G. Schreckenbach, *J. Phys. Chem. A* **2000**, *104*, 6259.
- [39] Z. Cao, K. Balasubramanian, *J. Phys. Chem.* **2005**, *123*, 114309.
- [40] E. B. Boys, F. Bernardi, *Mol. Phys.* **1970**, *19*, 553.
- [41] J. Ivanić, *J. Chem. Phys.* **2003**, *119*, 9364.
- [42] K. Andersson, P. Å. Malmqvist, B. O. Roos, A. J. Sadley, K. Wolinski, *J. Phys. Chem.* **1990**, *94*, 5483.
- [43] K. Andersson, P. Å. Malmqvist, B. O. Roos, *J. Chem. Phys.* **1992**, *96*, 1218.
- [44] P. G. Allen, J. J. Bucher, D. K. Shuh, N. M. Edelstein, T. Reich, *Inorg. Chem.* **1997**, *36*, 4676.
- [45] H. A. Thompson, G. E. Brown, Jr., G. A. Parks, *Am. Mineral.* **1997**, *82*, 483.
- [46] L. Helm, A. E. Merbach, *Chem. Rev.* **2005**, *105*, 1923.
- [47] J. Cooper, T. Ziegler, *Inorg. Chem.* **2002**, *41*, 6614.
- [48] T. Remsungnen, B. M. Rode, *Chem. Phys. Lett.* **2003**, *367*, 586.
- [49] R. Armunanto, C. F. Schwenk, A. H. Setiaji, B. M. Rode, *Chem. Phys.* **2003**, *295*, 63.
- [50] H. Eyring, *J. Chem. Phys.* **1935**, *3*, 107.
- [51] K. J. Laidler, M. C. King, *J. Phys. Chem.* **1983**, *87*, 2657.
- [52] E. Wigner, *J. Chem. Phys.* **1937**, *5*, 720.
- [53] I. F. Galván, M. E. Martín, M. A. Aguilar, *J. Comput. Chem.* **2004**, *25*, 1227.
- [54] S.-Y. Yang, I. Hristov, P. Fleurat-Lessard, T. Ziegler, *J. Phys. Chem. A* **2005**, *109*, 197.
- [55] D. Hagberg, G. Karlström, B. O. Roos, L. Gagliardi, *J. Am. Chem. Soc.* **2005**, *127*, 14250.
- [56] M. Druchok, T. Bryk, M. Holovko, *J. Mol. Liq.* **2005**, *120*, 11.
- [57] P. Carloni, M. Sprik, W. Andreoni, *J. Phys. Chem. B* **2000**, *104*, 823.
- [58] R. Armunanto, C. F. Schwenk, B. M. Rode, *J. Phys. Chem. A* **2003**, *107*, 3132.
- [59] W. L. Jorgensen, *Acc. Chem. Res.* **1989**, *22*, 184.
- [60] R. W. Impey, P. A. Madden, I. R. McDonald, *J. Phys. Chem.* **1983**, *87*, 5071.
- [61] T. S. Hofer, H. T. Tran, C. F. Schwenk, B. M. Rode, *J. Comput. Chem.* **2004**, *25*, 211.
- [62] C. F. Schwenk, M. J. Loferer, B. M. Rode, *Chem. Phys. Lett.* **2003**, *382*, 460.
- [63] S. Amira, D. Spångberg, K. Hermansson, *PhysChemChemPhys* **2005**, *7*, 2874.
- [64] C. F. Schwenk, B. M. Rode, *ChemPhysChem* **2003**, *4*, 931.
- [65] C. F. Schwenk, T. S. Hofer, B. R. Randolph, B. M. Rode, *PhysChemChemPhys* **2005**, *7*, 1669.
- [66] F. P. Rotzinger, *J. Phys. Chem. A* **2000**, *104*, 8787.

Received: November 28, 2005

Revised: June 22, 2006

Published online: October 18, 2006